Oxygen Transport Ceramic Membranes

Quarterly Report

July 2005 – September 2005

Principal Authors:

Prof. S. Bandopadhyay

Dr. T. Nithyanantham

Issued: November 2005

DOE Award # DE-FC26-99FT40054

University of Alaska Fairbanks
Fairbanks, AK 99775

Contributing sub contractors:

1. **X.-D Zhou, Y-W. Sin and H. U. Anderson,** Materials Research Center, University of Missouri-Rolla, Rolla, MO 65401
2. **Prof. Alan Jacobson and Prof. C.A. Mims;** University of Houston/University of Toronto

ABSTRACT

The present quarterly report describes some of the investigations on the structural properties of dense OTM bars provided by Praxair and studies on newer composition of Ti doped LSF.

In the current research, the electrical conductivity and Seebeck coefficient were measured as a function of temperature in air. Based on these measurements, the charge carrier concentration, net acceptor dopant concentration, activation energy of conduction and mobility were estimated.

The studies on the fracture toughness of the LSFT and dual phase membranes at room temperature have been completed and reported previously. The membranes that are exposed to high temperatures at an inert and a reactive atmosphere undergo many structural and chemical changes which affects the mechanical properties. To study the effect of temperature on the membranes when exposed to an inert environment, the membranes (LAFT and Dual phase) were heat treated at 1000°C in air and N_2 atmosphere and hardness and fracture toughness of the membranes were studied after the treatment. The indentation method was used to find the fracture toughness and the effect of the heat treatment on the mechanical properties of the membranes.

Further results on the investigation of the origin of the slow kinetics on reduction of ferrites have been obtained. The slow kinetics appears to be related to a non-equilibrium reduction pathway that initially results in the formation of iron particles. At long times, equilibrium can be reestablished with recovery of the perovskite phase.

2-D modeling of oxygen movement has been undertaken in order to fit isotope data. The model will serve to study “frozen” profiles in patterned or composite membranes.

TABLE OF CONTENTS

LIST OF GRAPHICAL MATERIALS

INTRODUCTION

Conversion of natural gas to liquid fuels and chemicals is a major goal for the Nation as it enters the 21st Century. Technically robust and economically viable processes are needed to capture the value of the vast reserves of natural gas on Alaska's North Slope, and wean the Nation from dependence on foreign petroleum sources. Technologies that are emerging to fulfill this need are all based syngas as an intermediate. Syngas (a mixture of hydrogen and carbon monoxide) is a fundamental building block from which chemicals and fuels can be derived. Lower cost syngas translates directly into more cost-competitive fuels and chemicals.

The currently practiced commercial technology for making syngas is either steam methane reforming (SMR) or a two-step process involving cryogenic oxygen separation followed by natural gas partial oxidation (POX). These high-energy, capital-intensive processes do not always produce syngas at a cost that makes its derivatives competitive with current petroleum-based fuels and chemicals.

In the mid 80's BP invented a radically new technology concept that will have a major economic and energy efficiency impact on the conversion of natural gas to liquid fuels, hydrogen, and chemicals.[1] This technology, called Electropox, integrates oxygen separation with the oxidation and steam reforming of natural gas into a single process to produce syngas with an economic advantage of 30 to 50 percent over conventional technologies.[2]

The Electropox process uses novel and proprietary solid metal oxide ceramic oxygen transport membranes [OTMs], which selectively conduct both oxide ions and electrons through their lattice structure at elevated temperatures.[3] Under the influence of an oxygen partial pressure gradient, oxygen ions move through the dense, nonporous membrane lattice at high rates with 100 percent selectivity. Transported oxygen reacts with natural gas on the fuel side of the ceramic membrane in the presence of a catalyst to produce syngas.

In 1997 BP entered into an OTM Alliance with Praxair, Amoco, Statoil and Sasol to advance the Electropox technology in an industrially sponsored development program. These five companies

---

[1]Mazanec, T. J.; Cable, T. L.; Frye, J. G., Jr.; US 4,793,904, 27 Dec **1988**, assigned to The Standard Oil Company (now BP America), Mazanec, T. J.; Cable, T. L.; US 4,802,958, 7 Feb **1989**, assigned to the Standard Oil Co. (now BP America), Cable, T. L.; Mazanec, T. J.; Frye, J. G., Jr.; European Patent Application 0399833, 24 May **1990**, published 28 November **1990.**

[2]Bredesen, R.; Sogge, J.; "A Technical and Economic Assessment of Membrane Reactors for Hydrogen and Syngas Production" presented at Seminar on the Ecol. Applic. of Innovative Membrane Technology in the Chemical Industry", Cetraro, Calabria, Italy, 1-4 May **1996**.

[3] Mazanec, T.J., *Interface*, **1996**; Mazanec, T.J., *Solid State Ionics*, 70/71, **1994** 11-19; "Electropox: BP's Novel Oxidation Technology", T.J. Mazanec, pp 212-225, in "The Role of Oxygen in Improving Chemical Processes", M. Fetizon and W.J. Thomas, eds, Royal Society of Chemistry, London, **1993**; "Electropox: BP's Novel Oxidation Technology", T.J. Mazanec, pp 85-96, in "The Activation of Dioxygen and Homogeneous Catalytic Oxidation", D.H.R. Barton, A. E. Martell, D.T. Sawyer, eds, Plenum Press, New York, **1993**; "Electrocatalytic Cells for Chemical Reaction", T.J. Mazanec, T.L. Cable, J.G. Frye, Jr.; Prep Petrol Div ACS, San Fran, **1992** *37*, 135-146; T.J. Mazanec, T.L. Cable, J.G. Frye, Jr.; *Solid State Ionics*, **1992**, 53-56, 111-118.

have been joined by Phillips Petroleum and now are carrying out a multi-year $40+ million program to develop and commercialize the technology. The program targets materials, manufacturing and engineering development issues and culminates in the operation of semi-works and demonstration scale prototype units.

The Electropox process represents a truly revolutionary technology for conversion of natural gas to synthesis gas not only because it combines the three separate unit operations of oxygen separation, methane oxidation and methane steam reforming into a single step, but also because it employs a chemically active ceramic material in a fundamentally new way. On numerous fronts the commercialization of Electropox demands solutions to problems that have never before been accomplished. Basic problems in materials and catalysts, membrane fabrication, model development, and reactor engineering all need solutions to achieve commercial success. Six important issues have been selected as needing understanding on a fundamental level at which the applied Alliance program cannot achieve the breadth and depth of understanding needed for rapid advancement. These issues include:

1. Oxygen diffusion kinetics (University of Houston);
2. Phase stability and stress development (University of Missouri - Rolla);
3. Mechanical property evaluation in thermal and chemical stress fields (University of Alaska Fairbanks)

Statement of Work

Task 1 *Evaluate phase stability and thermal expansion of candidate perovskite membranes and develop techniques to support these materials on porous metal structures.*

Task 2 *Determine materials mechanical properties under conditions of high temperatures and reactive atmospheres.*

Task 3 *Measure kinetics of oxygen uptake and transport in ceramic membrane materials under commercially relevant conditions using isotope labeling techniques.*

EXECUTIVE SUMMARY

Research on the Oxygen Transport Membranes as identified in tasks 1-3 are being performed at the various universities under the stewardship of Praxair. The quarterly technical report presents the progress of the tasks defined to understand the fundamental concepts and structural performance of the OTM material.

The conductivity measurements were made in air between 200 and 1200^{o}C using the D.C. four point probe electrical conductivity measurement method with four Pt wires as the contacts. Electrical conductivity and Seebeck coefficient of LSFT were measured as a function of temperature in air. A maximum conductivity of 12.5 S/cm was observed at 500^{o}C. At temperatures above 500^{o}C the electrical conductivity decreased and the Seebeck coefficient increased (indicating a decrease in charge carriers). On the other hand, below 500^{o}C the Seebeck coefficient remained essentially constant even though the electrical conductivity increased. This occurs because the conductivity is proportional to the product of the carrier concentration and the mobility.

The LSFT and dual phase membranes were heat treated at 1000°C for 60min and air and N_2 atmosphere. The Fracture toughness and hardness of the heat treated membranes were calculated using Vicker's indentation method and the effect of indentation load and atmosphere on the mechanical properties were studied. The crack propagation behavior and the fracture toughness values suggested that the inert atmosphere affects the fracture behavior significantly. The effect of loading time on the fracture toughness values is not so significant.

We have continued to investigate the thermodynamic properties (stability and phase-separation behaviour) and total conductivity of prototype membrane materials. The data are needed together with the kinetic information to develop a complete model for the membrane transport. We have previously reported characterization, stoichiometry, conductivity, and dilatometry measurements for samples of $La_{0.2}Sr_{0.8}Fe_{0.55}Ti_{0.45}O_{3-x}$. In this period, we have investigated by transmission electron microscopy the microstructure of ferrites that show very slow kinetics in the intermediate pressure range. The data suggest that the non-equilibrium behavior is associated with the formation of nano-particles of a reduced component which re-react at long times.

In the area of isotope transient studies at steady state, the current quarter has been dominated by extending modeling studies beyond 1-D analysis in order to properly analyze data from composite membranes or membranes with architecture which requires 2-D treatment.

Task 1: Preparation and Characterization of Dense Ceramic oxygen Permeable Membranes

X.-D Zhou[1], Q. Cai[2], J. Yang[1], W. B. Yelon[1], W. J. James[1] and H. U. Anderson[1]

1. **Materials Research Center, University of Missouri-Rolla, Rolla, MO 65401**
2. **Department of Physics, University of Missouri-Columbia, Columbia, MO 65211**

Conductivity and Seebeck coefficient of $La_{0.2}Sr_{0.8}Fe_{0.55}Ti_{0.45}O_{3-\delta}$ (LSFT) as a function of temperature

Experimental

$La_{0.2}Sr_{0.8}Fe_{0.55}Ti_{0.45}O_{3-\delta}$ (LSFT) powder was fabricated using the glycine-nitrate process and then pressed under the pressure of 10 ksi using a uni-axial press to make a pellet. The pellet was sintered at 1400°C for 5 hours. A rectangular bar (2.2 mm x 3.3 mm x 20 mm) was prepared from the pellet for the conductivity measurement.

The conductivity measurements were made in air between 200 and 1200°C using the D.C. four point probe electrical conductivity measurement method with four Pt wires as the contacts. A Keithley Model 2400 Series Source Meter was used as a constant current source and a Keithley 195A Digital Multi-meter was connected to a personal computer through the interface, which was used to measure the potential difference between the two inner Pt wires which were wrapped around the samples. Electrical conductivity and Seebeck coefficient of LSFT were measured as a function of temperature in air.

Results and Discussion

Figure 1 shows the plots of electrical conductivity and Seebeck coefficient as a function of temperature in air. A maximum conductivity of 12.5 S/cm was observed at 500°C. At temperatures above 500°C the electrical conductivity decreased and the Seebeck coefficient increased (indicating a decrease in charge carriers). On the other hand, below 500°C the Seebeck coefficient remained essentially constant even though the electrical conductivity increased. This occurs because the conductivity is proportional to the product of the carrier concentration and the mobility. Below 500°C, the Seebeck coefficient (carrier concentration) remains constant, but due to its exponential dependence on temperature, the mobility increases which causes the increase in

the conductivity. As the temperature increases above 500^{o}C, the electrical conductivity decreased because of the loss of oxygen which forms oxygen vacancies which act as donors to further decrease the charge carrier concentration. Even though the mobility continues to increase with temperature, its increase is less than the decrease in carrier concentration which leads to the maximum in electrical conductivity at 500^{o}C and the continuing decrease in conductivity with increasing temperature.

The concentration of charge carriers is related to the Seebeck coefficient by the relationship:

$$Q = \pm \frac{k}{e}[\ln(\frac{1-c}{c})] + \alpha^{*}$$

where Q is in mV/K or mV/C, k is Boltzmann's constant, c is the ratio of charge carriers to available conduction sites and α^{*} is a contribution arising from vibrational entropy of transport. In most cases of electronic transport, the magnitude of α^{*} is rather small and thus is negligible. Figure 2 shows a plot of the charge carrier concentration and Seebeck coefficient as function of temperature.

Since the Sr'_{La} acts as an acceptor, we expected the molar hole content to be 0.8. However, as can be seen in Figure 3, the net acceptor dopant concentration was found to be approximately 0.4. This low value occurs because the acceptor ($[Sr'_{La}]$) is compensated by the donor ($[Ti^{\bullet}_{Fe}]$), thus a lower hole concentration occurs because $p = [Sr'_{La}] - [Ti^{\bullet}_{Fe}]$. That is; due to the compensation, p = 0.8-0.45 or 0.35.

The activation energy of conduction and mobility were also estimated and plotted in Figure 4. The activation energy is 0.24 eV which implies that the LSCF has the small polaron conduction mechanism.

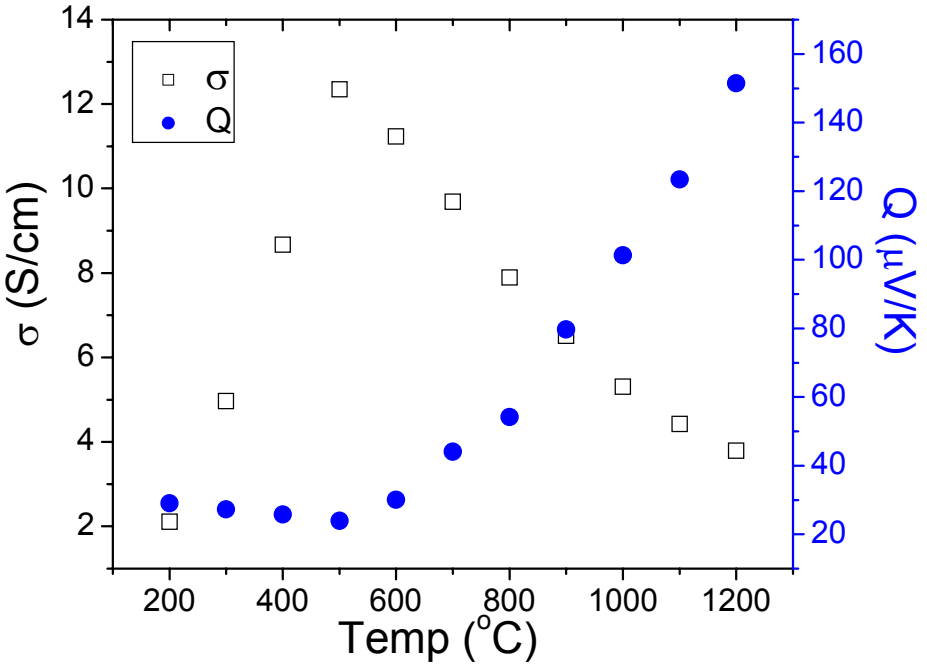

Figure 1 Electrical conductivity and Seebeck coefficient of LSFT as a function of temperature

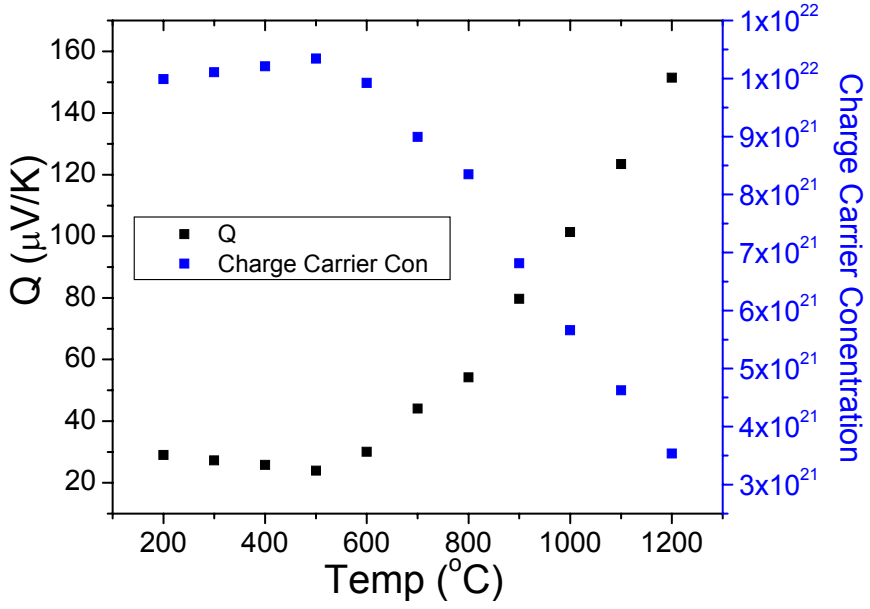

Figure 2 Charge carrier concentration and Seebeck coefficient of LSFT as a function of temperature

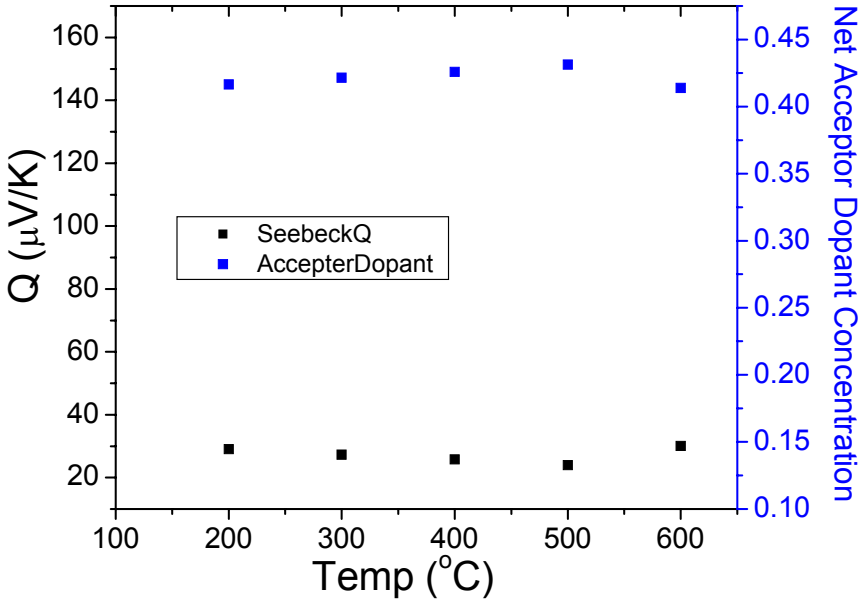

Figure 3 Net acceptor dopant concentration and Seebeck coefficient of LSFT as a function of temperature

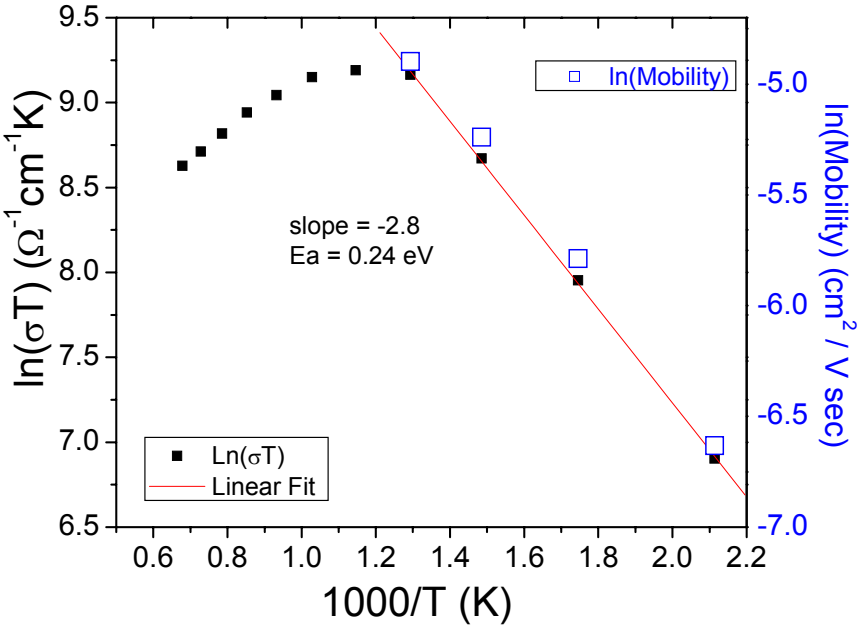

Figure 4 Ln(σT) vs. 1/T of LSFT and corresponding Mobility measured in air as a function of temperature

Future studies

1. Electrical conductivity and Seebeck coefficient will be measured as functions of oxygen activity and temperature.
2. TGA measurement will be carried out as function of oxygen activity and temperature.
3. From the conductivity data which will be collected in #1 along with the TGA data in #2, the defect chemistry of LSFT will be investigated.

TASK 2: Determine material mechanical properties under conditions of high temperature and reactive atmosphere

Prof. S. Bandopadhyay and Dr. T. Nithyanantham
University of Alaska Fairbanks, AK 99775

The studies on the fracture toughness of the LSFT and dual phase membranes at room temperature have been completed and reported previously. The membranes that are exposed to high temperatures at an inert and a reactive atmosphere undergo many structural changes which affects the mechanical properties of the membranes to a large extent. In order to study the effects of exposing the membrane at high temperature in an inert atmosphere, the membranes (LSFT and Dual phase) were heat treated at 1000°C in air and N_2 atmosphere and the hardness and fracture toughness of the membranes were studied after the heat treatment. The indentation method was used to find the fracture toughness. The effect of the heat treatment and the indentation load on the mechanical properties of the membranes was studied.

Experimental:

The LSFT and LSFT-CGO (dual phase) membranes were cut into small pieces and polished using polishing sheets and diamond pastes. The final polishing was carried out using 1μm diamond paste and the polished samples were used for heat treatment in the air and N_2 atmosphere. The temperature for the heat treatment was chosen as 1000°C and the air and N_2 (200ml/min) was chosen as the atmospheres. The samples were heated at the rate of 20°C/ min and dwelled at the maximum temperature for 60min prior to cooling to room temperature. The Vicker's indentation method was used to analyze the hardness and fracture toughness of the membrane. Four loads (100, 300, 500 and 1000g) were used for performing indentation and 10 and 30 seconds were used as two loading times at each load. The fracture toughness of the membranes was calculated using the equations of Niihara et al. (1982). Crack lengths were measured from the optical micrographs of the indentations and cracks. The l/a and c/a values were calculated to verify crack types. Appropriate formulas were used to calculate the fracture toughness and the results were compared. The equation suggested by Niihara et al. (1982) for the Palmqvist cracks ($0.25 \leq l/a \leq 2.5$) is given in equation 2.1.

$$\left(\frac{K_{IC}\,\Ø}{H\sqrt{a}}\right)\left(\frac{H}{E\Ø}\right)^{0.4} = 0.035(l/a)^{-0.5} \qquad \text{--- (2.1)}$$

and that for the median cracks ($c/a \geq 2.5$) is

$$\left(\frac{K_{IC}\,\Ø}{H\sqrt{a}}\right)\left(\frac{H}{E\Ø}\right)^{0.4} = 0.129\,(c/a)^{-1.5} \qquad \text{--- (2.2)}$$

where,

K_{IC} is the Mode I critical stress intensity factor (MPa.m ^{½})
Ø is the constraint factor (≈ 3.0)
H is the Vickers hardness (GPa)
E is the Young's modulus (GPa)
a is the half diagonal of the Vicker's indent (m)
c is the radius of the surface crack (median) (m) and
l is the crack length (Palmqvist) (m)

The Young's modulus of the materials was assumed to be 123GPa, where as, Ø is the constraint factor which is approximately 3.0 for ceramics.

Results and Discussion:

The hardness values of the LSFT which was heat treated at 1000°C in air and N_2 was shown in Figure 5. The effect of loading time on hardness is also shown in the figure. In general the hardness values decreases with increasing load.

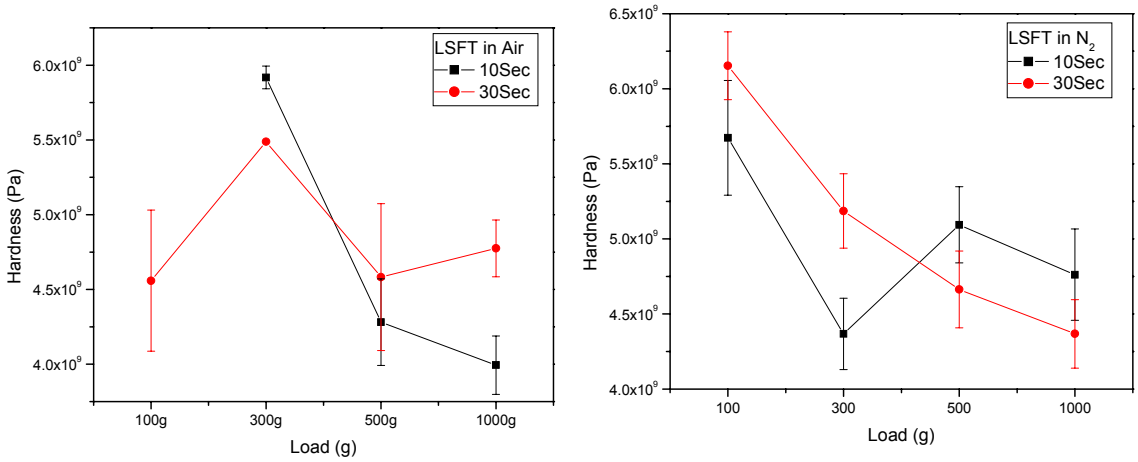

Figure 5. Dependence of hardness of the LSFT membrane on indentation load.

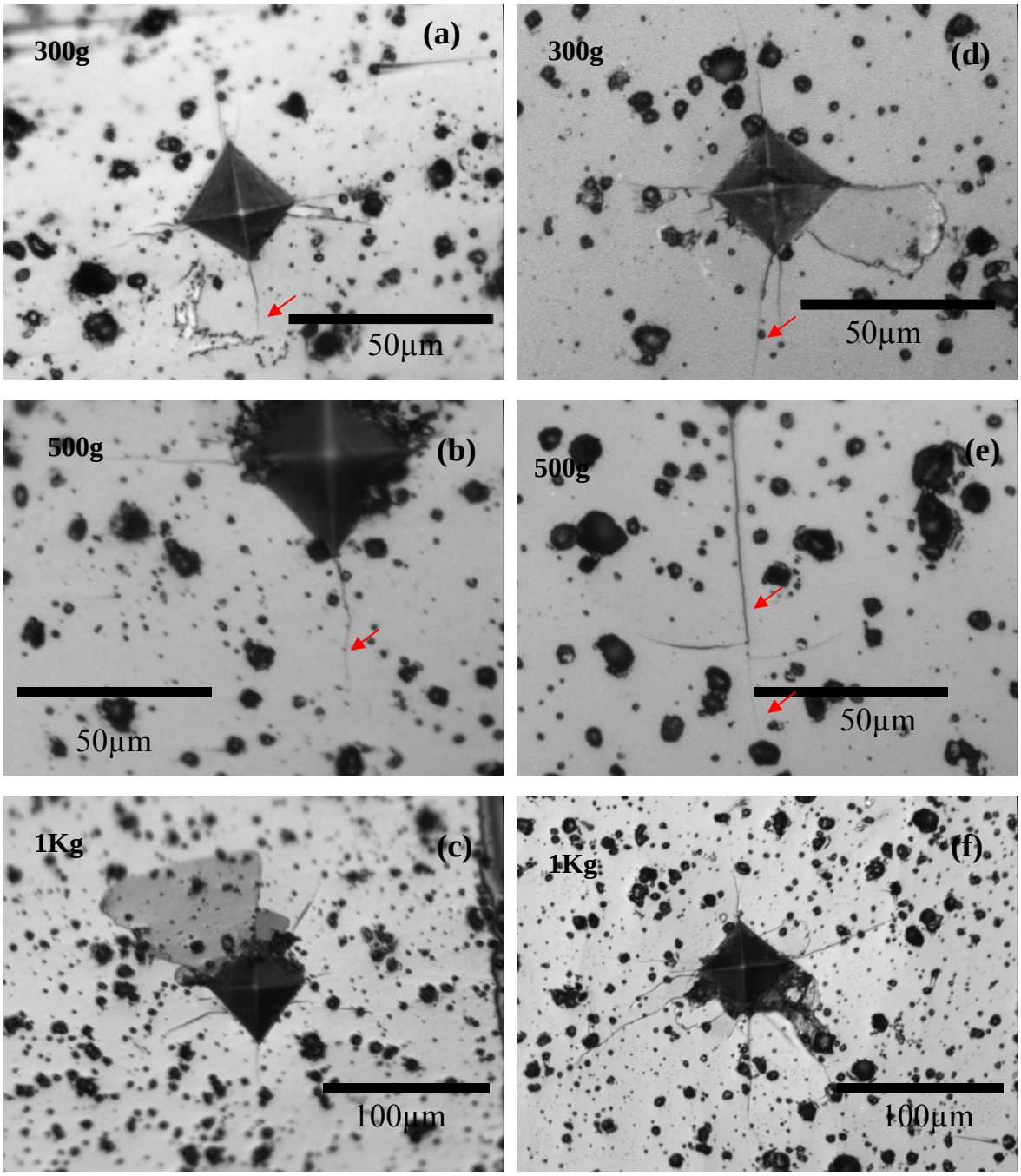

Figure 6 Optical micrographs of the indentation and cracks on LSFT membrane which was heat treated at 1000°C in air (a,b,c) and in N_2 atmosphere (d,e,f). The cracks that are generated in the N_2 treated samples are longer at the same load.

Figure 6 shows the optical micrographs of the indentation made at various loads on LSFT heat treated at 1000°C. The loading time was 10 Sec for all indentations shown in the figure. Figure 5 shows the dependence of hardness on indentation load. Closer observation of the load-Vicker's hardness curves suggests a transition, where hardness changes from load dependent to load independent. At lower loads, the indentation work is absorbed by volume deformation and by fracture surface formation processes. As the load is increased, the indentation becomes larger and more energy is consumed in both volume deformation and fracture surface generation process and number of crack types like median, radial and lateral cracks are formed during indentation process, depending upon indenter geometry, load, elasticity and microstructural behavior. In a brittle material like LSFT, after some critical load the fracture surface generation process consumes more energy and the volume deformation process is left unchanged. Hence the hardness remains almost the same after the critical load.

Figure 6 provides important information on the effect of atmosphere on crack generation and growth process. The cracks that are formed in the membranes which were heat treated in air are smaller than that of the cracks that are generated in the N_2 treated membranes (arrow marks). The number of crack initiations is also more in the N_2 treated membranes. This shows that the heat treatment in N_2 environment either transforms the microstructure significantly or forms new precipitates in along the grain boundaries.

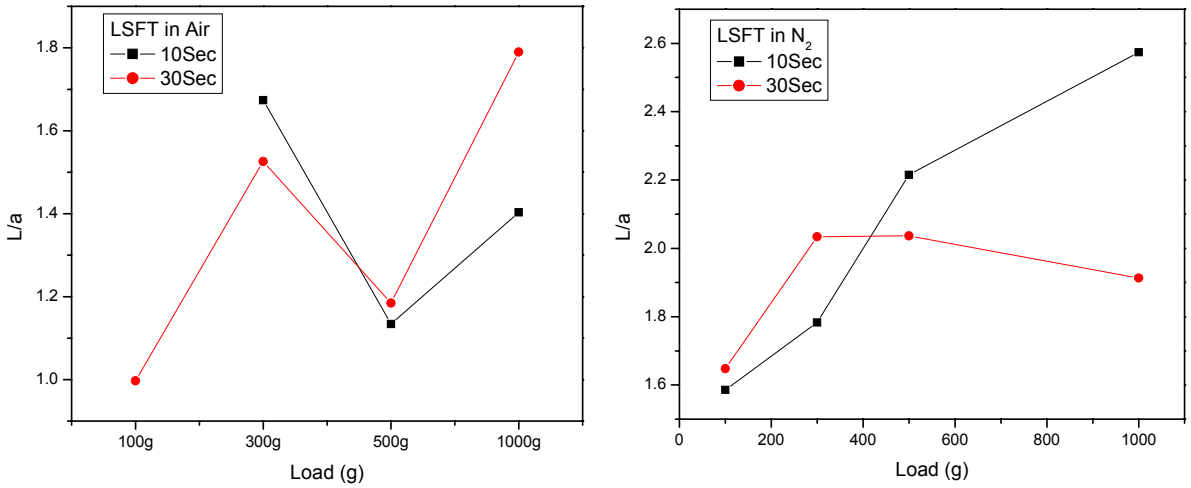

Figure 7: Dependence of L/a of LSFT on indentation load

.

The dependence of L/a of LSFT which was heat treated in air and N_2 atmosphere on indentation load is shown in Figure 7. The membranes treated in air shows no meaningful change with increasing indentation load but the L/a of the N_2 treated membrane increases with increasing indentation load. Moreover the L/a values for the N_2 treated samples are significantly higher than the air treated samples. Hence it is concluded that the treatment of LSFT in N_2 significantly alter the microstructure of the membranes. The structural and microstructural changes associated with the heat treatment have to be analyzed using x-ray diffraction analysis and SEM.

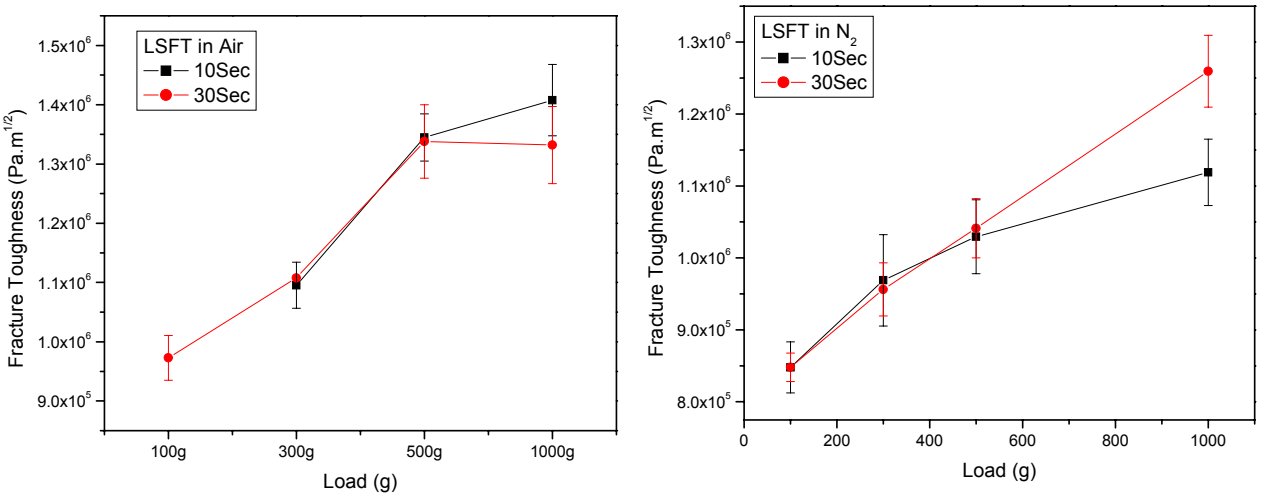

Figure 8: Dependence of fracture toughness of LSFT on indentation load

Fracture toughness of the LSFT is shown in the figure 8. In general, the fracture toughness values of the membranes increases with increasing indentation load. The fracture toughness of the LSFT heat treated in air, reaches a maximum fracture toughness value and remains mostly unchanged and also the fracture toughness value is higher than the K_{IC} value of N_2 treated sample. Even though the increment in the fracture toughness is consistence with the increasing load, the fracture toughness of membrane is reduced by the N_2 atmosphere.

The dependence of the hardness of dual phase samples is shown in Figure 9. The hardness of the dual phase membrane is significantly affected by the atmosphere in which it was heat treated. The hardness values of the air treated samples hardly changes with increasing indentation load but the hardness in the N_2 treated sample increases with increasing load. This is contrary to the behavior of the brittle materials. At a given load, the hardness of the N_2 treated membrane is slightly inferior to the air treated samples. This shows the inert atmosphere affects the structural behavior of the membrane when it was heat treated.

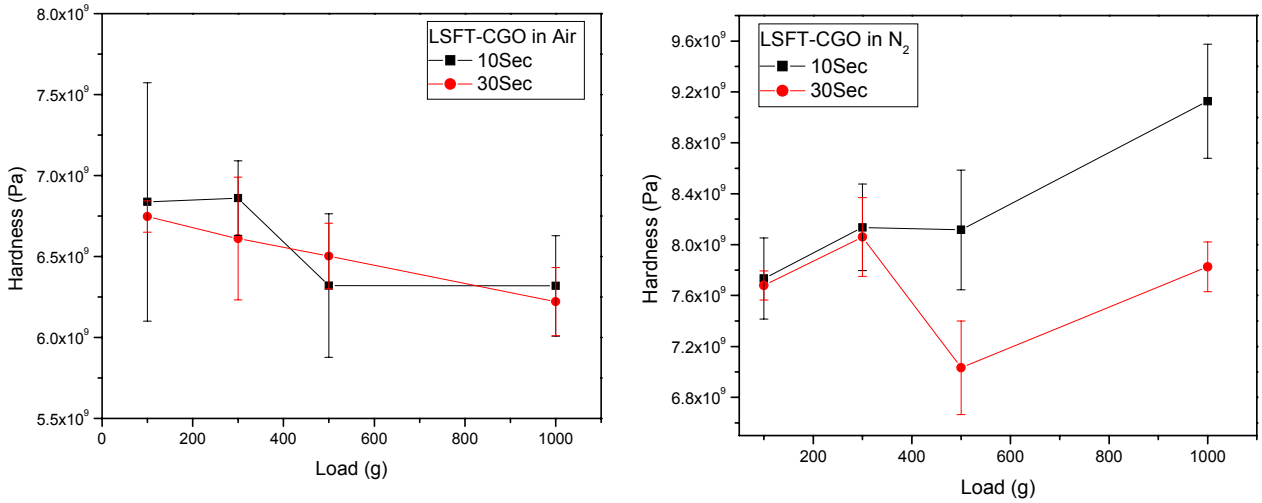

Figure 9: Dependence of the hardness of dual phase samples on indentation load

The dependence of L/a of dual phase membrane, treated in air and N_2 on the indentation is shown in Figure 7. The effect of loading time on the development of cracks is very much significant in the air treated samples, where as no such influence is observed in the N_2 treated samples. The L/a value increases with increasing load for the samples heat treated in N_2 atmosphere.

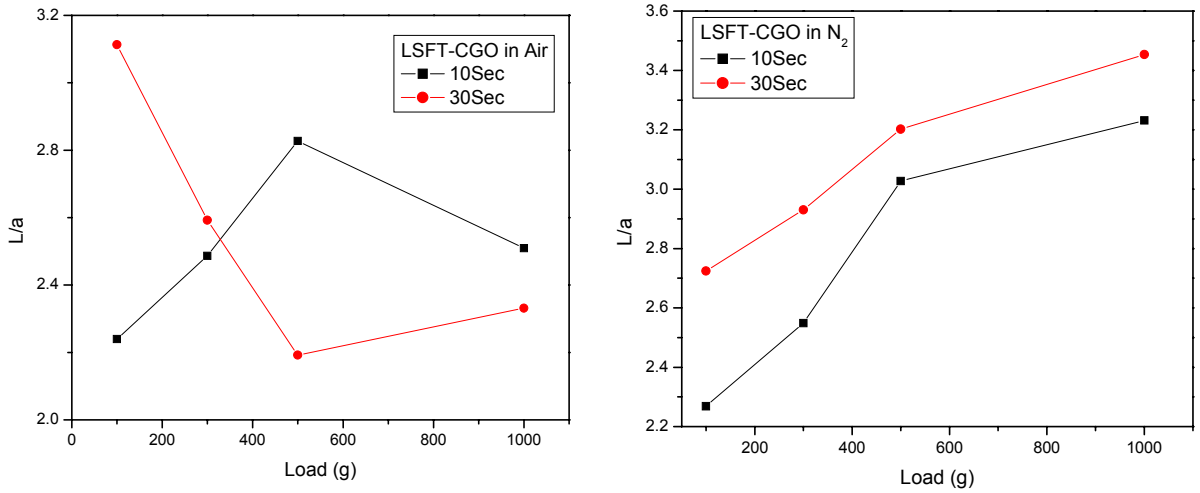

Figure 10: The dependence crack propagation of dual phase membrane on indentation load.

The optical micrographs of the indentations and cracks on dual phase membranes are shown in Figure 11. In the dual phase membrane, the crack propagation and hardness

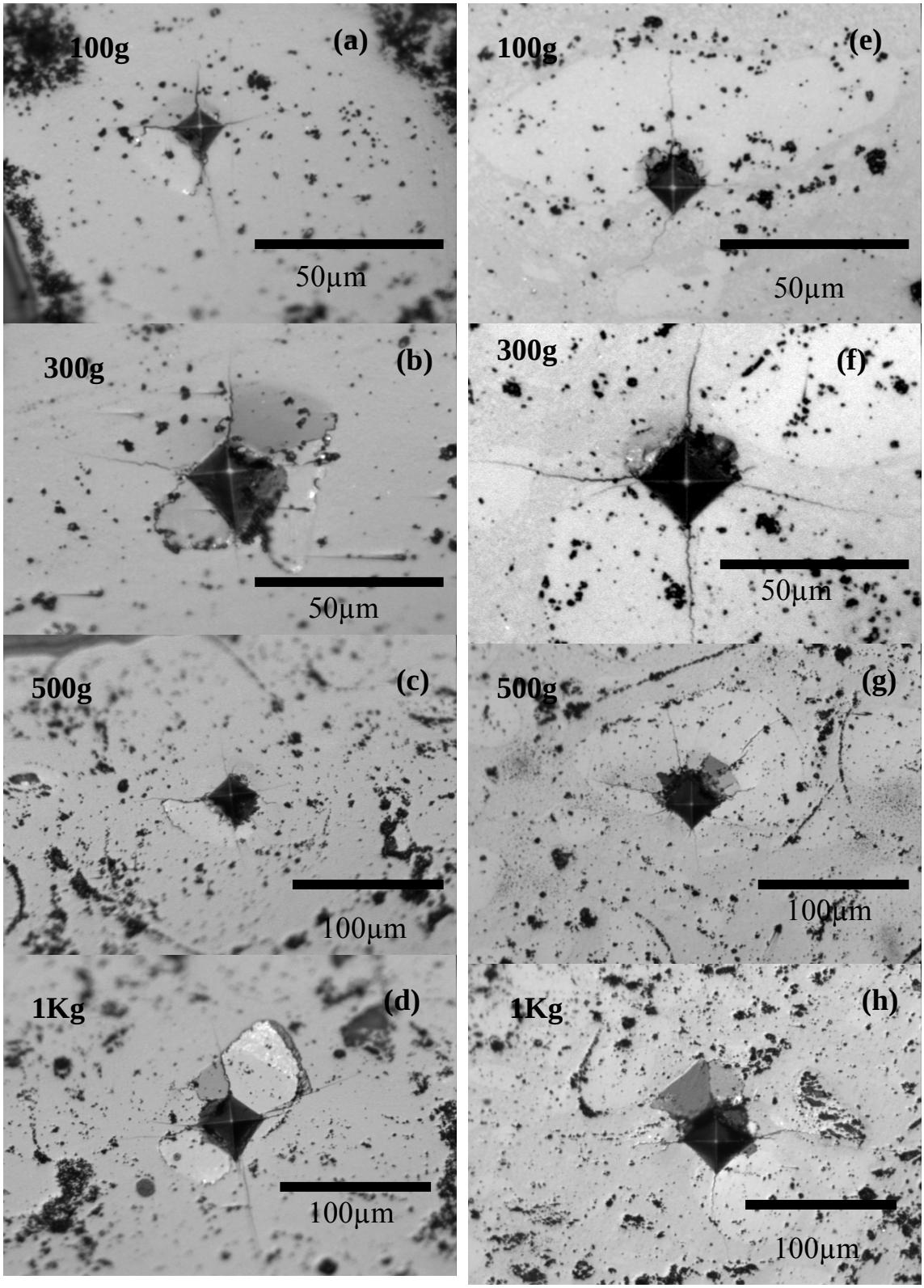

Figure 11: Optical micrographs of the indentation and cracks on dual phase membrane which was heat treated at1000°C in air (a,b,c,d) and N_2 atmosphere (e,f,g,h).

of the membrane are determined by the microstructural inhomogeneities. The crack propagation is affected by the continuous porous phase and the secluded dense phase. The effect of the dense and porous region on the crack propagation is clearly shown in the optical micrographs. The fracture toughness measurements are plotted in the Figure 12.

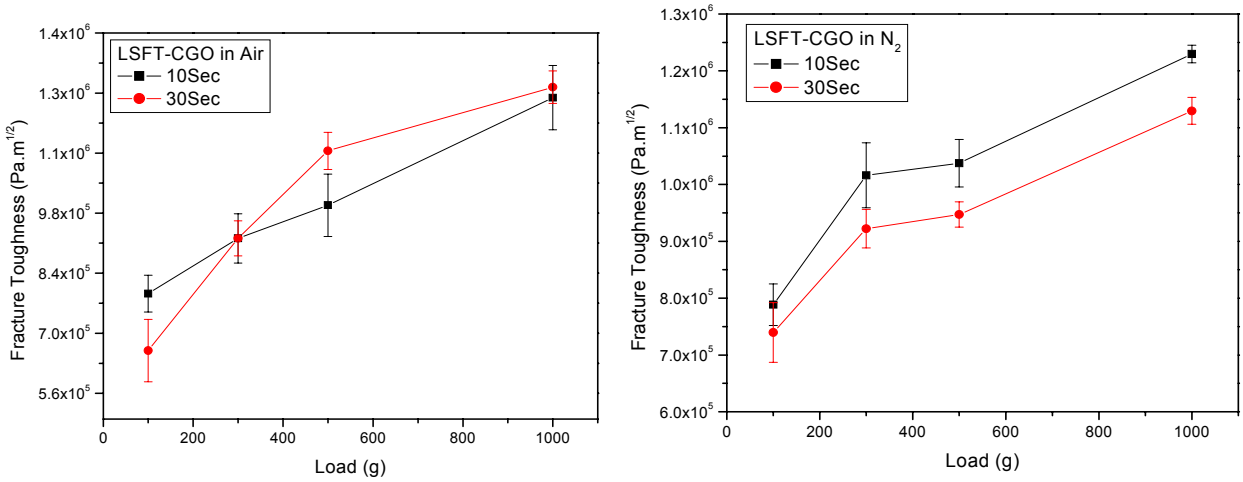

Figure 12: Dependence of fracture toughness of dual phase membrane on indentation load heat treated at 1000°C in air and N_2.

The fracture toughness values are found to be increasing with increasing load irrespective of the environment it was heat treated in. In accordance to the hardness values, the fracture toughness values of the N_2 treated samples are also slightly inferior to the values of the air treated dual phase membrane. The effect of indentation load or loading time has no significant effect on the fracture toughness values of this dual phase membranes.

Plans for next quarter:

- Dual phase sample preparation at Praxair facility
- Flexural strength studies on the dual phase membranes.
- X-ray diffraction and microstructural analysis of the air and N2 treated membranes.

Task 3: Measurement of Surface Activation/Reaction Rates in Ion Transport Membranes using Isotope Tracer and Transient Kinetic Techniques

A. J. Jacobson, University of Houston, C.A. Mims, University of Toronto

3.1 INTRODUCTION

The aim of this research project is to measure, using transient isotope tracing, chemical transients and other electrical measurements, key kinetic parameters related to surface activation/exchange rates for single phase mixed electronic ionic conductors and dual phase composites. The surface reaction rates together with the bulk transport kinetics can be used to model the production of synthesis gas from methane in a membrane reactor.

In principle, any part of an oxide membrane can experience oxygen activities which cover the entire range from the air to the fuel side. The entire solid will experience the conditions of the air side if the reaction of surface oxygen at the fuel side is rate limiting. In this case all regions of the membrane 'upstream' (towards the air side) can be in partial equilibrium with air. At the other extreme, if oxygen activation is rate limiting, the entire solid operates under the reducing conditions of the fuel side. If oxygen transport through the solid is rate limiting, then a gradient across the solid between the two extremes is present. All of the key kinetic parameters, surface reaction rates, oxygen diffusion, and conductivity depend on the oxygen activity.

Modeling the performance of a membrane device involves solving the coupled continuity equations. To date, published models have assumed constant properties (for example, a simple first order rate constant for oxygen surface activation and a single value of the diffusion coefficient). Clearly, if the surface and bulk transport rates have a strong dependence on the oxygen activity, these models will contain significant errors and will not provide reliable predictions especially when the pO_2 gradient is large as is the case for syn gas generation. As illustrated above the distribution of the pO_2 gradient

depends on the relative rates of the surface and bulk processes and consequently kinetic data for the whole range of partial pressures is relevant.

In this program, we use several key techniques in order to collect the necessary data for the understanding of the transport properties of perovskite oxide membranes. At the University of Houston, transport properties are measured by measuring the transient uptake of oxygen using electrical conductivity relaxation, coupled with precise measurements of oxygen stoichiometry and DC conductivity. At the University of Toronto, isotopic tracing methods are used to measure transport properties – (1) isotope exchange depth profiling (IEDP) and (2) transient isotope tracing of operating membranes.

3.2 EXPERIMENTAL

Most of the work at UH this quarter has been directed towards experiments on the non-equilibrium behavior of $La_{0.2}Sr_{0.8}Fe_{0.55}Ti_{0.45}O_{3-\delta}$. Samples of this composition prepared and characterized as previously reported were quenched in pellet form from a series of oxygen partial pressures at 900 ºC. The pO_2 values were 1.25×10^{-4} atm, 1.11×10^{-7} atm, 1.70×10^{-10} atm, and 6.74×10^{-14} atm. After the quench X-ray patterns were recorded. The X-ray patterns show little or no evidence for other than a pure perovskite phase. Similar experiments were carried out for $La_{0.5}Sr_{0.5}FeO_{3-x}$ A sample was air-quenched from 850 °C and $pO_2 = 10^{-8}$ to 10^{-9} atm. A second sample was treated in $5\%H_2/N_2$ for two successive periods of 24 and 48 h.

Specimens for electron microcopy study were prepared from the quenched samples by cutting slices, polishing and the thinning using a Gatan ion mill. The samples were examined in a JEOL 2020F high resolution transmission electron microscope.

The other experimental techniques used to generate the results reported here have been described in previous quarterly reports

3.3 RESULTS AND DISCUSSION

University of Houston

Non-equilibrium behavior

We have continued to investigate the thermodynamic properties (stability and phase-separation behavior) and total conductivity of prototype membrane materials. The data are needed together with the kinetic information to develop a complete model for the membrane transport. We have previously reported characterization, stoichiometry, conductivity, and dilatometry measurements for samples of $La_{0.2}Sr_{0.8}Fe_{0.55}Ti_{0.45}O_{3-x}$. In this report, we describe further investigations of the non-equilibrium behavior observed in conductivity and thermal expansion previously reported. Similar extremely slow equilibrium kinetics have also been observed in other ferrites including $La_{0.5}Sr_{0.5}FeO_{3-x}$ and we have gone back to study the behavior of this composition. The general features of the behavior are shown in Figure 2.

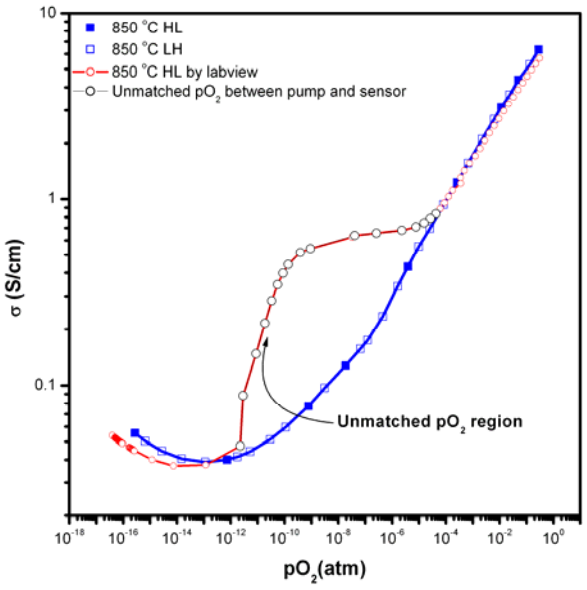

Figure 13. Conductivity measurements for LSFTO showing the non-equilibrium behavior in the intermediate pressure range.

An understanding of this behavior is needed to predict membrane performance on pO_2 cycling. To address the question, we have examined quenched samples by high resolution transmission electron microscopy. Samples of LSTO in the form of dense ceramic disks were quenched from different pO_2 values that span the range of behavior from 900 ºC. Preliminary results indicate significant differences in microstructure for the samples quenched from the different partial pressures. Results for the sample quenched from 1.25×10^{-4} atm are shown in Figure 3. The sample was observed to have two distinct microstructures. In one region, the sample has the perovskite structure with very few defects but in other regions the sample was quite different. A low magnification image of region 2 is shown in Figure 3. In addition to the grain boundary, the microstructure contains many small (~ 5-10 nm domains) that are roughly circular. At higher resolution these regions are clearer and can be seen to be crystalline. Detailed analysis of the structure of the central particle by Fourier inversion gives a lattice constant that corresponds to iron metal and not to that of any iron oxide phases. The current model based on these results is that the perovskite phase has an easy kinetic pathway to reduction that eliminates oxygen vacancies by forming metallic iron. We propose a general mechanism as indicated below

$ABO_3 \rightarrow ABO_{3-x} \rightarrow A_2BO_4 + AO \rightarrow A_2BO_4 + B$ or alternatively $ABO_3 \rightarrow ABO_{3-x} \rightarrow$ 'ABO_x' $+AO \rightarrow$'ABO_x' $+B$ where 'ABO_x' is an amorphous phase.

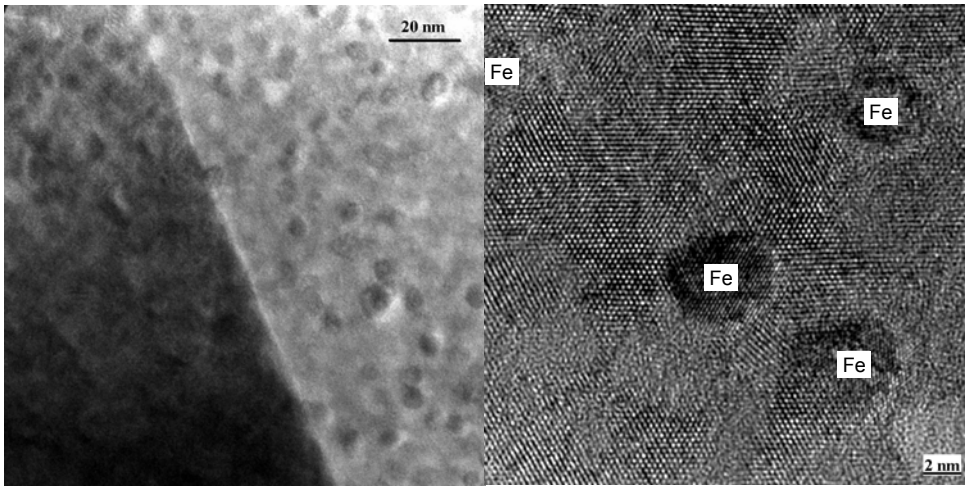

Figure 14. Electron micrographs of region 2 in the structure of LSFTO quenched from 900 °C and $pO_2 = 1.25 \times 10^{-4}$ atm.

We see no evidence in the microstructure as yet for the presence of the 214 phase so the second mechanism may be more likely.

We note the recent observation that in thin film synthesis of $La_{0.5}Sr_{0.5}FeO_{3-x}$, the phases formed under reducing conditions are 214 $LaSrFeO_4$ and Fe. We have examined this composition in bulk form to compare the results with the thin film data. The results are shown in Figure 4 below. A sample was heated at 950 °C in 5% H_2/N_2 and then quenched. At this stage the onset of decomposition was apparent and the sample contained the perovskite phase together with $LaSrFeO_4$ together with Fe metal. Heat treatment for a further 24 h resulted in complete conversion to $LaSrFeO_4$ and Fe metal.

Other examples of processes that occur in perovskite oxides on the introduction of large vacancy concentrations are known. For example reduction of $LaCoO_3$ at 673 K using Zr metal gives two distinct phases occur, namely $La_2Co_2O_5$ and $La_3Co_3O_8$. $La_2Co_2O_5$ oxidizes via $La_3Co_3O_8$ to $LaCoO_3$. $La_2Co_2O_5$ and $La_3Co_3O_8$ are metastable, and undergo irreversible decomposition reactions to CoO and the Ruddlesden–Popper type phases $La_{m+1}Co_mO_{3m+1}$, m=1 and 3, upon heating under inert atmosphere. Presumably under more reducing conditions Co metal would be formed.

In the Co, the oxygen vacancy phases are metastable with respect to the Ruddlesden–Popper phases and this may also be the case for $La_{0.5}Sr_{0.5}FeO_{2.75}$. In compounds with other substituents or compositions particularly those that stabilize the perovskite structure, we propose similar reactions occur but they do not correspond to the equilibrium phase assembly. Instead the non equilibrium situation reactions occur locally and not throughout he sample. In the region where Fe^{2+} concentration is still small it is kinetically favorable to change the stoichiometry as shown by the equation:

$$La_{0.5}Sr_{0.5}FeO_{2.75} \rightarrow La_{0.5}Sr_{0.5}FeO_{2.75-\delta}(1-\delta/3) \rightarrow La_{0.5}Sr_{0.5}FeO_{2.75-\delta} + \delta/3LaSrFeO_4 + \delta/3Fe$$

The reaction occurs only locally and with enough time at a fixed pO_2 and temperature equilibrium will be restablished.

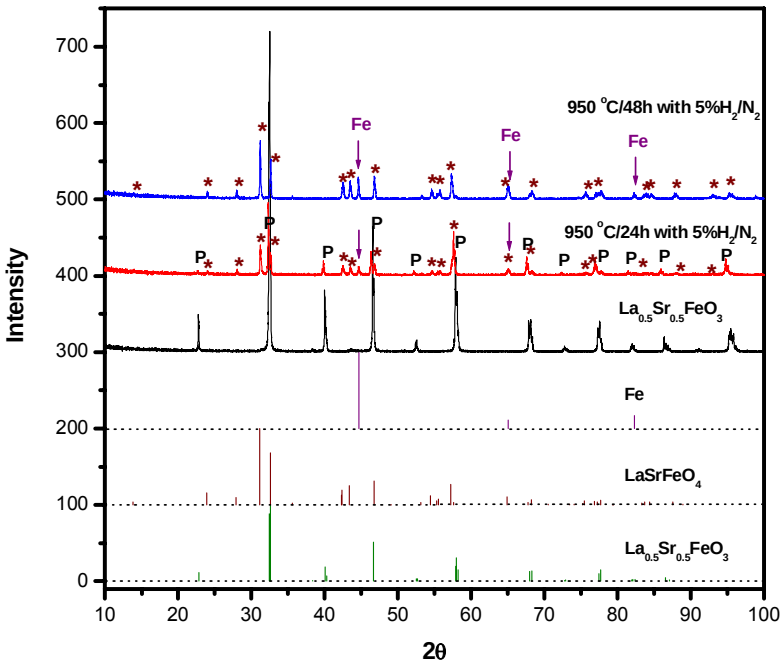

Figure 15. Powder X-ray diffraction spectra of $La_{0.5}Sr_{0.5}FeO_{3-\delta}$ and the reduction products together with reference spectra.

3.4 Plans for next quarter

In the next quarter, we will begin an investigation of some dual phase systems.

3.5 University of Toronto

Isotope Studies

Materials can be examined in the absence of an oxygen potential gradient by isotope exchange depth profiling at a particular condition. As set forth in previous reports, the various surface and bulk transport parameters can be separately determined on an operating membrane by the application of an isotopic transient (a pulse of $^{18}O_2$ in our case) on one side of an operating membrane and the subsequent time dependence of ^{18}O evolution from both sides of the membrane. Both the forward and reverse surface rates can be directly measured. In flux measurements, only the net rates are available. Many such experiments can be performed on one sample, thus removing the sample-to-sample

variability in IEDP experiments. The parameters under a large gradient have been seen to differ from those under gradientless conditions.

Summary of progress:

Modelling efforts

In the previous report, the ^{18}O SIMS profile from an LSCrF membrane under high oxygen gradient conditions, with a CO/CO_2 mixture on the outside and 20% oxygen on the inside of the membrane, and which was quenched during an isotope transient experiment was presented and analyzed. One of the significant findings is that a proper fit of the data, which showed a marked asymmetry in the traveling isotopic wave, required non-uniform bulk oxygen diffusivity in the model. A fourfold increase in the oxygen diffusivity across the membrane is consistent with the data. Such a gradient is consistent with oxygen stoichiometry changes which accompany the broad range in oxygen potential in this experiment. The fits were obtained stochastically by hand, with a chosen gradient modified by trial and error until an acceptable fit emerged. In the past quarter, we have begun to build more general models. The aspects under study include the following.

Non-linear membrane behavior: A full defect model has been assembled which uses the thermodynamic information obtained by the Houston group to adjust the local defect density as part of the differential mass balance. This model will be linked to various models of the surface reactivity in order to reproduce the apparent bistable flux condition which was seen in the previous isotope transients on the LSCrF membrane.

Two dimensional isotope tracing: A two dimensional model is being assembled both in FEMLAB and in C. The need for extra dimensionality in our experiments arises from two different features. The first is the need for a 2-D treatment of the gas phase under high flux conditions. The oxygen partial pressure can be substantially reduced on the air side as the gas flows along inside of the tube. More significant is the change in CO/CO_2 ratio on the delivery side as the product gas flows along the outside annular space. One

explanation of the apparently bistable operation is that the surface rates have a strong dependence on the local oxidation potential. Particularly, it appears that the reduced perovskite oxide surface is more active for CO oxidation than a more oxidized surface. As mentioned in the previous report, the separation of small domains of iron metal could be involved in this drastic change in kinetics. This model will be run to try to obtain insight into the bistable behavior. As a result of axial changes in the gas phase composition, the quenched isotope transient could show axial variations in the "frozen" isotope wave. A weak axial variation was seen in the ^{18}O profile figure in the quenched LSCrF membrane previously reported. The peak ^{18}O fraction at the top of the figure is 5% while at the bottom the maximum is 5.5%. Part of this can arise from the distribution of isotope during the transient because of changes in reversibility at various conditions. Axial heterogeneity in this sample is obviously mild, but for longer tubes and substantial conversion of the gas, 2-D modeling will be necessary to obtain the distributed flux conditions from the resulting frozen isotope distribution. More interesting is

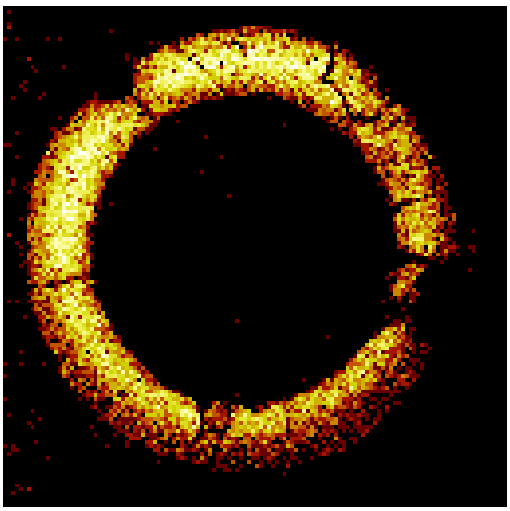

Figure 16: ^{18}O map of LSCrF tube cross section.

the possibility of radial distribution in performance. The reassembled membrane appears to have a variation in the radius of maximum ^{18}O content as one proceeds around the tube. At the lower right, the peak appears closer to the inner wall than in the upper portion. This would indicate lower than average flux in the lower portion.

The other use of the 2-D model is the planned investigation of composite membrane materials where oxygen flow through desired heterogeneities can be traced to examine the role of grain boundaries, etc.

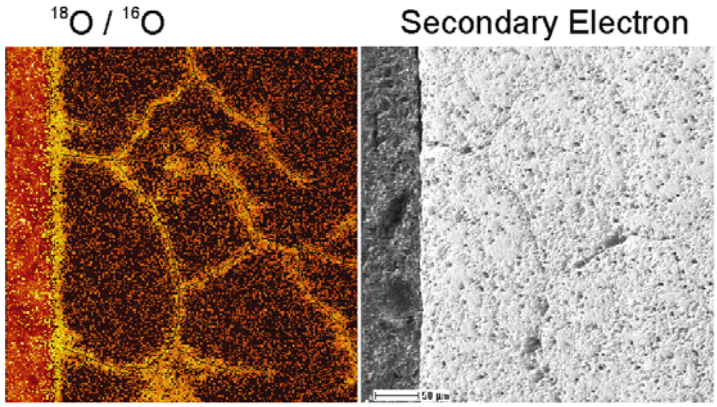

Figure 17: ^{18}O maps of infused $PrBaCo_2O_{5+x}$ samples sintered from powders.

In recent investigations of cobalt-containing perovskites, heterogeneities and internal porosity were observed in IEDP and are shown in the figure below. Some of the ^{18}O rich veins correspond to apparent cracks in the material. Others do not. The narrow profiles bordering the darker zones can be analyzed for the k and D values of these regions, and macroscopic transport through the porosity can be independently measured on the same sample. We will pursue such studies in the composite membrane materials.

The local value of Do at steady state is governed by the vacancy concentration which is governed by the local chemical (oxygen) potential (in the case of high electronic conductivity). This is not expected to yield a linear variation in Do. We have begun work on a simultaneous defect/transport model which will incorporate the previously measured thermodynamic oxygen stoichiometry data and will report on this in the next quarter.

Membrane reactor improvements:

The transient membrane reactor was refurbished for experiments scheduled in the next period. The reactor has been located nearer to the mass spectrometer in order to

enable the study of significantly more rapid isotope transients. Such rapid transients are expected in some of the composite materials and supported films.

3.6 Plans for the next quarter:

Modelling: Further analysis of previously infused samples will be pursued with the 2-D model.

Isotope tracing: Composite materials chosen by consultation with partners will analyzed by IEDP. This will include patterned or layered materials. The membrane reactor will be reassembled with either LSFTO or a composite membrane.

Publications and Presentation:

J. Yoo, A. Verma, S. Wang, A. J. Jacobson, "Oxygen transport kinetics in $SrFeO_{3-x}$, $La_{0.5}Sr_{0.5}FeO_{3-x}$, and $La_{0.2}Sr_{0.8}Cr_{0.2}Fe_{0.8}O_{3-x}$ measured by electrical conductivity relaxation". Journal of the Electrochemical Society (2005), 152(3), A497-A505.

N. Bayani, C.A. Mims, A.J. Jacobson, and P.A.W. van der Heide, "Modes of surface exchange in $La_{0.2}Sr_{0.8}Cr_{0.2}Fe_{0.8}O_{3-d}$" Solid State Ionics (2005) 176(3-4) 319-323.

C. Y. Park and A. J. Jacobson, "Electrical Conductivity and Oxygen Non-stoichiometry of $La_{0.2}Sr_{0.8}Fe_{0.55}Ti_{0.45}O_{3-\delta}$", Journal of the Electrochemical Society (2005) in press.

C. Y. Park and A. J. Jacobson, "Thermal and chemical expansion properties of $La_{0.2}Sr_{0.8}Fe_{0.55}Ti_{0.45}O_{3-x}$" Solid State Ionics accepted.

Two talks (one keynote) were presented at the International Solid State Ionics conference in Baden-Baden Germany July 2005.

CONCLUSIONS

The conductivity measurements were made in air between 200 and 1200^{o}C using the D.C. four point probe electrical conductivity measurement method with four Pt wires as the contacts. Electrical conductivity and Seebeck coefficient of LSFT were measured as a function of temperature in air. A maximum conductivity of 12.5 S/cm was observed at 500^{o}C. At temperatures above 500^{o}C the electrical conductivity decreased and the Seebeck coefficient increased (indicating a decrease in charge carriers). On the other hand, below 500^{o}C the Seebeck coefficient remained essentially constant even though the electrical conductivity increased. This occurs because the conductivity is proportional to the product of the carrier concentration and the mobility.

The LSFT and dual phase membranes were heat treated at 1000°C for 60min and air and N_2 atmosphere. The Fracture toughness and hardness of the heat treated membranes were calculated using Vicker's indentation method and the effect of indentation load and atmosphere on the mechanical properties were studied. The crack propagation behavior and the fracture toughness values suggested that the inert atmosphere affects the fracture behavior significantly. The effect of loading time on the fracture toughness values is not so significant. The structural changes caused by the atmosphere has to be analyzed using x-ray diffraction and SEM.

We have continued to investigate the thermodynamic properties (stability and phase-separation behaviour) and total conductivity of prototype membrane materials. The data are needed together with the kinetic information to develop a complete model for the membrane transport. We have previously reported characterization, stoichiometry, conductivity, and dilatometry measurements for samples of $La_{0.2}Sr_{0.8}Fe_{0.55}Ti_{0.45}O_{3-x}$. In this period, we have investigated by transmission electron microscopy the microstructure of ferrites that show very slow kinetics in the intermediate pressure range. The data suggest that the non-equilibrium behavior is associated with the formation of nano-particles of a reduced component which re-react at long times.

In the area of isotope transient studies at steady state, the current quarter has been dominated by extending modeling studies beyond 1-D analysis in order to properly analyze data from composite membranes or membranes with architecture which requires 2-D treatment.

REFERENCES:

N/A

BIBLIOGRAPHY **N/A**

LIST OF ACRONYMS AND ABBREVIATIONS

YSZ	Yttria stabilized zirconia
XRD	X-ray diffraction
$La_{0.2}Sr_{0.8}Fe_{0.55}Ti_{0.45}O_{3-\delta}$	LSFTO
IEDP	Isotope exchange and depth profiling
SIMS	Secondary Ion Mass Spectroscopy